表4　クロイツフェルト・ヤコブ病診断基準

・診断確実例（definite）
特徴的な病理所見を有する例，又はウエスタン・ブロット法や免役染色法で脳に異常なプリオンタンパクを検出し得た症例．（新変異型では，ウエスタン・ブロット法にて英国の症例と同一パターンが検出される）

・診断ほぼ確実例（probable）
病理所見がない症例で，進行性痴呆を示し，脳波で PSD を認める．更にミオクローヌス，錐体路 / 錐体外路障害，小脳症状，視覚異常，無動性無言のうち2項目以上を示す症例．（新変異型では英国例と臨床・病理像が同一であるが，脳組織のウエスタン・ブロット法が未検索）

・診断疑い例（possible）
診断ほぼ確実例と同じ臨床症状を示すが，PSD を欠く症例

スが観察され，大脳と小脳皮質に PrP^{Sc} は斑状や塊状に強く染まり，広汎に観察される．

診　　断

sCJD の診断基準は表4に示すようなものでプリオン病の確定診断は脳生検を行うか病理解剖を待たなければならない．そのため一般的には経過や MRI などの検査により臨床診断される．

1．画像診断

最近では MRI などの撮影技術の進歩により画像診断の有用性が高まっている．特に CJD の早期診断には MRI の拡散強調画像（DWI）が有用であるとされる[14]（図5）．以前は T2 強調画像で両側対称性の線条体の（大脳皮質に比して）高信号であることが画像診断のポイントだとされてきたが，この所見は軽微で発症早期では陰性になることがある．それに比べ DWI では従来の検査方法では所見が得られないような発症早期から信号が得られることがある．主として大脳皮質や線条体に明瞭な高信号を認める．基底核のうち淡蒼球は侵されず，視床では信号変化を認めることがある．初期の高信号は通常非対称性であるが経過とともに高信号領域は拡大し両側性になり，大脳皮質と線条体にも出現し，末期には比較的対称性となる．Demaerel らは sCJD で病理所見を確認したうえで，DWI は感度・特異度・陽性的中率共に 100 % と報告している[15]．

このように sCJD の診断には DWI のみで多くの情報を得られる

図5 クロイツフェルト・ヤコブ病（CJD）患者のMRI拡散強調画像

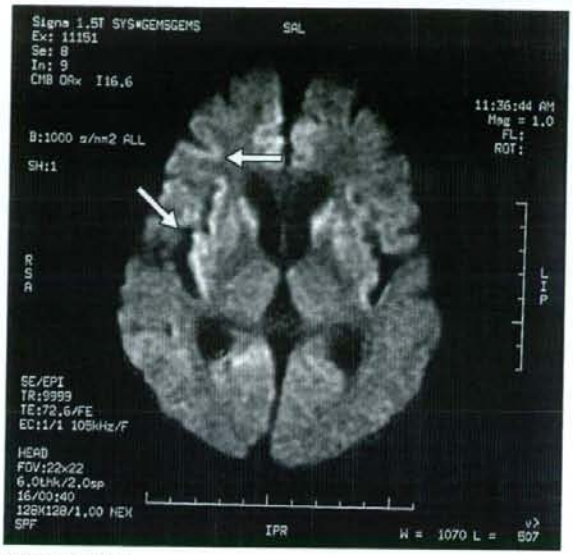

矢印が高信号域
（長崎大学，佐藤克也先生提供）

が，施設間の撮影方法や画像処理方法の違いが診断率に影響してくるため現在標準化が進められている．また，その他のプリオン病や他疾患との鑑別のためにT1，T2，proton densityのみでなく脳脊髄液抑制反転回転法（FLAIR）や，みかけの拡散係数（ADC）mapなどを含めたMRIを施行するとより確実である．

2．脳脊髄液診断マーカー

sCJDにおける髄液中の14-3-3タンパクの検出は特異度・感度共に90％に近くWHOの診断基準にも採用されている（表4）．しかし，この値は髄液の採取時期などによっても変動し発症初期では検出感度が低く，また発症後1年以上経った場合でも感度が70％以上と再び低下する．また，CJDのType 2ではType 1よりも検出感度は低いとされ，一度検出できなかったケースでも2週間後や1ヵ月後に調べると検出できるようになるなど病型や病気の進行によって検査結果が変動する．髄液中の14-3-3タンパクは橋本病脳症や代謝性疾患の一部，時には筋萎縮性側索硬化症などでも増加することがあ

るので，それらの疾患にも注意が必要である．一方，髄液中の総 tau タンパクも CJD で増加するものの1つである．この特異度・感度も 90％ 以上とされ 14－3－3 タンパクと同等である．総 tau タンパクはアルツハイマー型痴呆や脳血管性痴呆などでも上がってくるが，これはリン酸化 tau タンパクと総 tau タンパクとの比をとることで，特にアルツハイマー型痴呆を区別することが可能と報告されている[16]．

3．脳　波

病初期には高振幅性徐波を示し，次いで PSD が徐々に観察されてくるが末期には低振幅性の徐波だけになる．

4．その他のプリオン病の診断

1）遺伝性プリオン病の診断

遺伝性プリオン病は多数の表現型を示すため現在のところ，臨床的な診断基準はない．神経症状と共にプリオンタンパクの遺伝子変異が証明されたものは“ほぼ確実例（possible）”，病理変化まで確認されれば“確実例（definite）”と分類される．家族性あるいは遺伝性と呼ばれているが，遺伝的浸透率が低く家族歴がないものがあること，同一変異・同一家族であっても表現型が変わってくることがあることには注意を要する[17]．

2）硬膜移植 CJD の診断

従来の MRI では sCJD と大差はないが，DWI では移植硬膜近傍から高信号が広がるとされる．緩徐進行の非典型群では脳波で PSD が陰性あるいは末期出現し，髄液 14－3－3 タンパクは典型群に比べて陽性率などが低いなど診断に有用な異常所見の出現率も低いことが知られている．

3）変異型 CJD（vCJD）の診断

診断基準を表5に示すが，重要なのは MRI である．T2，proton density，FLAIR，DWI で両側の視床枕に視床枕兆候（pulvinar sign）と呼ばれる高信号が見られ，診断上の感度 90％，特異度 95％ 以上とされる[20]．また，中枢神経以外の末梢リンパ組織に PrP^{Sc} 質の蓄積が見られ扁桃生検も有用である．髄液検査では 14－3－3 タンパク陽性率は約半数で，総 tau タンパク上昇はさらに高頻度に見られると言う．

表5　変異型 CJD（vCJD）の診断基準（WHO2001）

Ⅰ	A．進行性の神経精神症状
	B．6ヵ月以上の病気の経過
	C．通常の検査で他の疾患が除外できる
	D．明らかな医原性原因への暴露病歴がない
	E．家族性 CJD を否定できる
Ⅱ	A．初期の精神症状（うつ状態，不安，無感情，妄想）
	B．持続性の疼痛性感覚異常
	C．失調
	D．ミオクローヌス，舞踏様運動，またはジストニア
	E．認知症
Ⅲ	A．脳波所見が孤発性 CJD の典型像である PSD を示さない
	B．MRI で両側の視床枕の高信号域
Ⅳ	A．扁桃生検で異常型プリオンタンパク陽性

診断確実例（definite）：IA および特徴的な神経病理学的所見
ほぼ確実例（probable）：Ⅰ＋Ⅱの5項目中4項目以上＋ⅢA＋ⅢB，
　　またはⅠ＋ⅣA
診断疑い例（possible）：Ⅰ＋Ⅱの5項目中4項目以上＋ⅢA

5．診断に関する研究動向

プリオン病の最終診断では Proteinase K 抵抗性の PrP^{Sc} の検出が一般的で疾患特異性は高いが検出感度は低く，また検体として主に中枢神経組織生検を要するため生前診断は難しい．近年，PrP^{Sc} を試験管内増幅させる方法（protein misfolding cyclic amplification：PMCA）を用いて微量の PrP^{Sc} を検出する試みが国内外で盛んに行われている[18]．これにより血液や髄液，尿などから微量 PrP^{Sc} を増幅し検出することにより発症前診断も可能になるかも知れない．

治　　療

プリオン病に対して有効な薬物療法はまだない．動物実験などの結果から治療の可能性が報告されているものとしてキナクリン／キニーネやペントサンポリサルフェイト（PPS），フルピリチンなどがある．キナクリンやキニーネは一過性に脳機能を回復するとされるが，肝障害などの副作用が強いため積極的には使用しない．PPS は本邦でも脳室内投与が実施されたが亜急性の症例では明らかな臨床的改善は示していない．アミロイド結合性低分子化合物や PrP 特異的に結合す

る低分子化合物の研究開発が勧められており発症予防効果を示すものが見つかっているが，実用段階にはほど遠いのが現状である．

ワクチンの開発も試みられてはいるが PrP^C はヒトゲノムにコードされているため1次構造を同じくする PrP^{Sc} は免疫寛容を起すためワクチンを作製することは難しいとされている．抗体療法は動物実験モデルにて有効性が示されたが，脳内へ移行性の問題など実用化までのハードルは高い．

予　　防

プリオン病は日常的な接触による感染の危険性はないとされる．したがってほかの感染症と同じく標準予防策で十分である（スタンダード・プレコーションでも“標準”扱いである）．非侵襲の医療行為に用いる各種内視鏡検査，血管内や尿道へのカテーテル挿入，循環呼吸機能検査に使う器具が接触するほとんどの臓器では感染性が検出されないので，これらにおいても特別な注意は必要ないと思われる．医原性の感染は生体材料と手術器具にて起っている．まず，生体材料としては血液・脳脊髄液が最も扱う頻度が高いと思われる．脳脊髄液に関しては感染性を持つ場合があるので分析は自動機器などでは行わずほかの使い捨ての物を使って調べるべきで，これに接触した用具は焼却するか，表6の方法で汚染除去しなければならない．手術器具による感染を防ぐためには，可能な限り，使い捨ての用具を使用し，使い捨てでない器具はすべて表面を廃棄可能な膜などで覆って使用するなどが考えられる．感染性組織に暴露した器具は可能な限り破棄するか，表6のうちその器具が耐えられる最も強力な汚染除去が必要になる[19]．血液に関しては，vCJD が輸血で感染するという報告があり[20]，スクリーニング検査法の開発が急務である．プリオン病の感染因子は，普通一般に用いられている消毒や滅菌方法などに抵抗性を示すうえ，乾燥やアルコール，ホルマリンでの固定により安定化し感染性が強くなることが知られている．さらに，感染性物と非感染の物を同一プール（液体）で保存しただけで非感染の物に汚染が広がることさえある．したがって，汚染の可能性のある物は厳密に隔離されたうえ，固定薬には暴露せず，取り扱うときから汚染除去薬に浸すまでの間は湿潤を

表6 伝達性海綿状脳症（TSE）に関する汚染除去法

Ⅰ．焼却

・すべての使い捨ての器具，用具，廃棄物に用いられる．

・高感染性の組織に暴露された機器のすべてに対して望ましい方法

Ⅱ．耐熱性の機器に対するオートクレーブ/化学的汚染除去法

(1)．1規定（1N）の水酸化ナトリウム（NaOH）に浸し，121℃，30分のオートクレーブで加熱し，汚染除去して水ですすぎ，通常の滅菌を受けさせる．

(2)．1N NaOHまたは次亜塩素酸（漂白剤，ブリーチ，20,000 ppmの塩素を供与できる濃度）に1時間浸し，器具を水に移し，121℃，1時間のオートクレーブで加熱後，汚染除去し，通常の滅菌を受けさせる．

(3)．1N NaOHまたは次亜塩素酸に1時間浸し，水で洗浄し，その後水浴に移して，121℃か132℃のオートクレーブで加熱，汚染除去し通常の滅菌を受けさせる．

(4)．1N NaOHに浸し，大気圧で10分間煮沸し，汚染除去して水ですすぎ，通常の滅菌を受けさせる．

(5)．次亜塩素酸（望ましい）または1N NaOH（代わりに）に常温で1時間浸し，汚染除去して水ですすぎ，通常の滅菌を受けさせる．

(6)．132℃，18分間オートクレーブ（表面についた乾燥した組織には効果は完全ではない）．

Ⅲ．熱不耐性の機器ないし表面に対する化学的汚染除去法

(1)．2N NaOHまたは希釈されていない次亜塩素酸に浸す．そのまま1時間保ち，その後拭き取り水ですすぐ．

(2)．表面がNaOHまたは次亜塩素酸に耐えられない場所は，徹底的に洗浄することで，希釈効果によるほぼ完全な汚染除去が期待できる．また，不完全な汚染除去剤を用いることで付加的汚染除去効果が得られるかも知れない．

Ⅳ．乾燥物に対するオートクレイブ/化学的汚染除去法

(1)．1N NaOHまたは次亜塩素酸に耐えられる小型の乾燥した物品は，前述したうちの1つあるいは他の溶液に最初に浸し，それから121℃以上，1時間のオートクレーブで加熱処理すべきである．

(2)．大型の乾燥した物品ないし1N NaOHまたは次亜塩素酸に耐えられない様々なサイズの乾燥した物品は，132℃，1時間のオートクレーブで加熱処理すべきである．

最も確実な汚染除去法は焼却処分であるが，処分できないものはその種類に応じてⅡ，Ⅲ，Ⅳから適する汚染除去法を選ぶ．(1)～(6)までの番号は，若い順に強力な方法なので，その施設に応じて最も強力な汚染除去法を選ぶべきである．

保つべきである．在宅看護において患者排泄物などへの特別な処置は必要ない．

おわりに

臨床および病理学的知見を中心にヒトプリオン病について概説してきた．ヒトプリオン病は遺伝性と感染性という2つの疾患概念が交差する特異な疾患群でありいまだ解明されていない部分も多い．ほかの

多くの神経変性疾患と共通して，異常化したタンパク質の脳内蓄積が病因の中心と考えられるコンフォメーション病としてプリオン病，あるいはアミロイドーシスの1つとしてプリオン病をとらえることもできる．また，ウイルス様の多様な病原株が存在し，人獣共通感染症の1つとして重要な疾患であり，vCJD と BSE 問題は医療現場のみならず畜産・食肉業界でも大きな問題となったことは記憶に新しい．幸い本邦では BSE 牛の発症数は少なく，vCJD は非典型例1例が報告されたのみにとどまっているが，英国を中心とする欧州では vCJD キャリアーが多くいることを想定し，医療行為による2次感染の危険性をいかに小さくするかが課題になっている．感染性タンパク粒子プリオンという概念が提唱されて20年を超えるが，「プリオン仮説は真実なのか」という根本的な命題には我々はまだ完全には答えきれていない．病因病態の解明だけではなく，治療法・ワクチンの開発，簡便な洗浄不活化法など解決しなければならない研究課題は多く残されている．最後に本稿執筆にあたり，貴重な臨床および病理データを供出していただいた佐藤克也先生（長崎大学・神経内科学）に感謝する．

文　　献

1) Parchi P, et al: Molecular basis of phenotypic variability in sporadic Creutzfeldt-Jakob disease. Ann Neurol 39 (6): 767-778, 1996.
2) Ladogana A, et al: Mortality from Creutzfeldt-Jakob disease and related disorders in Europe, Australia, and Canada. Neurology 64 (9): 1586-1591, 2005.
3) 厚生労働科学研究費補助金難治性疾患克服研究事業: プリオン病及び遅発性ウイルス感染に関する調査研究, 2007.
http://prion.umin.jp/result/yamadama.html
4) Hitoshi S, et al: Double mutations at codon 180 and codon 232 of the PRNP gene in an apparently sporadic case of Creutzfeldt-Jakob disease. J Neurol Sci 120 (2): 208-212, 1993.
5) Meiner Z, et al: Familial Creutzfeldt-Jakob disease. Codon 200 prion disease in Libyan Jews. Medicine (Baltimore) 76 (4): 227-237, 1997.
6) Brown P, et al: Phenotypic characteristics of familial Creutzfeldt-Jakob disease associated with the codon 178Asn PRNP mutation. Ann Neurol 31 (3): 282-285, 1992.
7) Gambetti P, et al: Conclusions of the symposium. Brain Pathol 8 (3): 571-575, 1998.

8) Zeidler M, et al: New variant Creutzfeldt–Jakob disease: neurological features and diagnostic tests. Lancet 350 (9082): 903–907, 1997.
9) 田丸恒美, 他: プリオン病の病理－硬膜移植後 CJD, 変異型 CJD を含めて. 神経進歩 47: 91–99, 2003.
10) 天野直二, 他: CJD の神経病理 CJD と vCJD の神経病理. Clinic Neurosci 24 (3): 322–326, 2006.
11) Budka H: Histopathology and immunohistochemistry of human transmissible spongiform encephalopathies (TSEs). Arch Virol Suppl (16): 135–142, 2000.
12) Hoshi K, et al: Creutzfeldt–Jakob disease associated with cadaveric dura mater grafts in Japan. Neurology 55 (5): 718–721, 2000.
13) 佐々木健介, 他: CJD の病理学的評価基準. Clinic Neurosci 24 (3): 327–330, 2006.
14) 藤田浩司, 他: CJD の画像診断. Clinic Neurosci 24 (3): 317–320, 2006.
15) Demaerel P, et al: Diffusion–weighted MRI in sporadic Creutzfeldt–Jakob disease. Neurology 52 (1): 205–208, 1999.
16) Satoh K, et al: Total tau protein in cerebrospinal fluid and diffusion–weighted MRI as an early diagnostic marker for Creutzfeldt–Jakob disease. Dement Geriatr Cogn Disord 24 (3): 207–212, 2007.
17) 山田正仁, 他: CJD と vCJD の現行診断基準と問題点. Clinic Neurosci 24 (3): 301–306, 2006.
18) Saborio G P, et al: Sensitive detection of pathological prion protein by cyclic amplification of protein misfolding. Nature 411 (6839): 810–813, 2001.
19) 山口尚宏, 他: クロイツフェルト・ヤコブ病対策. 麻酔科診療プラクティス 15: 58–61, 2004.
20) Wroe S J, et al: Clinical presentation and pre–mortem diagnosis of variant Creutzfeldt–Jakob disease associated with blood transfusion: a case report. Lancet 368 (9552): 2037–2039, 2006.

Overview of the human prion diseases

Naohiro Yamaguchi, Takayuki Fuse,
Daisuke Ishibashi, Ryuichiro Atarashi,
Noriyuki Nishida

Division of Cellular and Molecular Biology,
Department of Molecular Microbiology and Immunology,
Nagasaki University Graduate School of Biomedical Sciences

Simplified ultrasensitive prion detection by recombinant PrP conversion with shaking

To the editor: A key problem in managing prion diseases is the lack of a rapid, practical assay for prions (infectivity) at low-level infectious, or sub-infectious, amounts. Prion diseases involve the accumulation of a pathological, typically protease-resistant form of prion protein, termed PrP^{Sc}, which appears to propagate itself in infected hosts by inducing the conversion of its normal host-encoded precursor, PrP-sen, into additional PrP^{Sc} (refs. 1–4). In crude brain homogenates, PrP^{Sc} and infectivity can be amplified from endogenous PrP-sen during multiple rounds of intermittent sonication and serial dilution into fresh normal brain homogenate[2,4]. This ultrasensitive assay, termed PMCA, allows detection of ~1 ag of PrP^{Sc} in ~3 weeks[5].

To improve the speed and practicality of prion detection assays, we recently developed a cell-free conversion reaction that supports sustained PrP^{Sc}-seeded conversion of recombinant PrP-sen (rPrP-sen) to specific protease-resistant (rPrP-res) forms. This method (which we previously reported in *Nature Methods*), called rPrP-PMCA, uses periodic sonication and serial reaction rounds of the PMCA method, but is faster[6]. To circumvent problems associated with sonication in the PMCA and rPrP-PMCA methods (see **Supplementary Results** online), we have now developed a new prion assay, abbreviated QUIC for quaking-induced conversion, which uses rPrP-sen as a substrate and automated tube shaking rather than sonication. This assay can detect about one lethal prion dose within a day, and is faster and simpler than previous described PMCA[6] and rPrP-PMCA[5] assays.

Initial testing of QUIC reaction conditions revealed that periodic shaking enhanced PrP^{Sc}-seeded conversion of hamster rPrP-sen (residues 23–231) into PK-resistant conversion products (rPrP-$res^{(Sc)}$, where (Sc) refers to seeding by PrP^{Sc}; **Supplementary Fig. 1** and **Supplementary Methods** online). Consistent with our previous observations with rPrP-PMCA reactions[6], the rPrP-$res^{(Sc)}$ reaction products had 17-, 13-, 12- and 11-kDa fragments, which represented different C-terminal PrP fragments (**Supplementary Fig. 2** online). These results showed that periodic shaking could substitute for sonication in promoting rPrP-$res^{(Sc)}$ formation.

Additional experiments revealed that rPrP-$res^{(Sc)}$ generation was also sensitive to rPrP-sen concentration, reaction volume (**Supplementary Fig. 1**), reaction time (**Supplementary Fig. 2**), number of serial reactions (**Supplementary Fig. 3** online), temperature (**Supplementary Fig. 4** online) and shaking cycle (**Supplementary Results**). In QUIC reactions performed at 45 °C, we observed rPrP-$res^{(Sc)}$ formation in single 46-h QUIC reactions seeded with ≥100 ag of PrP^{Sc} (**Fig. 1a**). In contrast, 21 negative control reactions seeded with comparable dilutions of normal brain homogenate or buffer alone produced no rPrP-res (**Fig. 1b**). We obtained results similar to those shown in **Figure 1a,b** in an independent repeat experiment done in triplicate (data not shown). When we diluted products of PrP^{Sc}-seeded reactions 1,000-fold into fresh rPrP-sen to seed the subsequent reaction rounds, we observed strong propagation of rPrP-$res^{(Sc)}$ through at least 4 serial reactions (**Supplementary Fig. 5** online).

Elevation of QUIC reaction temperatures accelerated rPrP-$res^{(Sc)}$ formation. At 55 °C, we detected rPrP-$res^{(Sc)}$ in single 8-h reactions seeded with as little as 10 fg PrP^{Sc} (~2 lethal intracerebral doses; **Supplementary Fig. 4**). We detected 1 fg in 18-h reactions (**Supplementary Fig. 6** online). At 65 °C, we detected 100 fg PrP^{Sc} seed with a 4-h reaction (**Supplementary Fig. 4**). However, at 65 °C, there was also

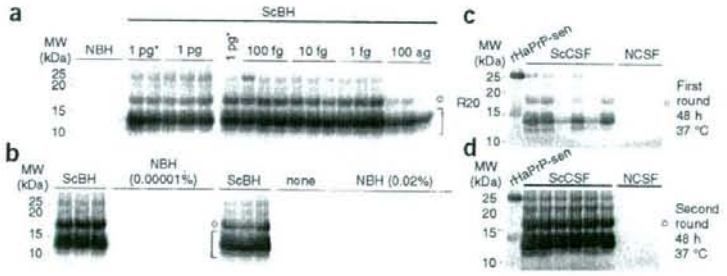

Figure 1 | QUIC reactions seeded with brain homogenates and CSF samples from normal or scrapie-affected hamsters. (**a**) Single-round 46-h, 45 °C QUIC reactions were seeded with dilutions of normal brain homogenate (NBH) and scrapie brain homogenate (ScBH) as described in **Supplementary Methods** online. Circles designate the 17-kDa rHaPrP-$res^{(Sc)}$ band and brackets designate the position of the ≤13 kDa rHaPrP-$res^{(Sc)}$ bands. QUIC sensitivity was determined by seeding with ScBH dilutions containing the indicated amounts of PrP^{Sc}. The NBH was 0.00001% (wt/vol) in the reaction, which is equivalent to that of the ScBH seed dilution containing 1 pg of PrP^{Sc}. We diluted the NBH and ScBH in 1% N-2 media supplement, except for the reactions marked 1 pg*, which were diluted with 0.1% N-2. (**b**) Multiple negative controls were performed under the conditions as in **a**. The ScBH seeds contained 1 pg of PrP^{Sc} and the indicated amounts of NBH. We seeded the lanes marked none with the diluent for the brain homogenates, N-2. (**c**,**d**) We seeded QUIC reactions with 2 µl CSF taken from normal hamsters ($n = 3$) or hamsters in the clinical phase of scrapie ($n = 6$). The reactions contained 0.05% SDS and 0.05% Triton X-100. We shook the QUIC reactions for 10 s every 2 min. PK-digested products of the first 48-h round were immunoblotted with antibody R20 (**c**). Second-round reactions were seeded with 10% of each first-round reaction volume and analyzed as in **c** (**d**). The leftmost lanes show 100 ng rHaPrP-sen without PK treatment.

more rapid formation of a distinct spontaneous product, rPrP-res$^{(spon)}$ (ref. 6), in reactions seeded with normal brain homogenate. Overall, there was a tradeoff between sensitivity and speed in QUIC assays, and, at any given temperature, the longer the total reaction time, the greater was the likelihood of rPrP-res$^{(spon)}$ formation.

Because cerebral spinal fluid (CSF) is a more accessible biopsy specimen than brain, we compared QUIC seeding activity in CSF samples collected from scrapie-affected hamsters or uninfected controls. After one 48-h round (at 37 °C), we saw no rHaPrP-res in the control reactions. However, all of the scrapie CSF reactions produced the rHaPrP-res$^{(Sc)}$ banding pattern with variable intensities (**Fig. 1c,d**). After a second serial QUIC reaction, control reactions still lacked rPrP-res, but the reactions seeded with scrapie CSF produced strong patterns consistent with the presence of rHaPrP-res$^{(Sc)}$. Similar two-round QUIC reactions showed that CSF samples from 10 additional uninfected control hamsters yielded no rHaPrP-res bands, but 2 of the original scrapie-positive CSF samples again yielded strong rHaPrP-res$^{(Sc)}$ (data not shown). Thus, QUIC reactions seeded with CSF samples discriminated between uninfected and scrapie-affected hamster CSF samples.

These observations suggest that a diagnostic test for prion infections based on CSF or other non-brain tissues or excretia may be possible. Further studies will be required to demonstrate the adaptability of the QUIC reaction to the detection of prions in other types of samples and to prion diseases of clinical and agricultural relevance. The relative speed, sensitivity, simplicity and ease of duplication of QUIC reactions should offer practical advantages in the development of prion assays.

Note: Supplementary information is available on the Nature Methods website.

ACKNOWLEDGMENTS

We thank G. Baron, V. Sim and L. Taubner for critical review of this manuscript. We thank K. Meade-White and B. Race (Rocky Mountain Laboratories) for the CSF samples, G. Raymond (Rocky Mountain Laboratories) for the brain tissue samples, and G. Hettrick and A. Mora for graphics assistance. This research was supported in part by the Intramural Research Program of the US National Institute of Allergy and Infectious Diseases, National Institutes of Health.

COMPETING INTERESTS STATEMENT

The authors declare competing financial interests: details accompany the full-text HTML version of the paper at http://www.nature.com/naturemethods/.

Ryuichiro Atarashi[1,2], Jason M Wilham[1], Leah Christensen[1], Andrew G Hughson[1], Roger A Moore[1], Lisa M Johnson[1], Henry A Onwubiko[1,3], Suzette A Priola[1] & Byron Caughey[1]

[1]Laboratory of Persistent Viral Diseases, National Institute for Allergy and Infectious Diseases, National Institutes of Health, Rocky Mountain Laboratories, 903 S. 4th St., Hamilton, Montana 59840, USA. [2]Department of Molecular Microbiology and Immunology, Nagasaki University Graduate School of Biomedical Sciences, 1-12-4 Sakamoto, Nagasaki 852-8523, Japan. [3]Present address: Department of Biochemistry, University of Nigeria-Nsukka, Nsukka, Enugu State, Nigeria.

e-mail: bcaughey@nih.gov

1. Kocisko, D.A. *et al. Nature* **370**, 471–474 (1994).
2. Castilla, J., Saa, P., Hetz, C. & Soto, C. *Cell* **121**, 195–206 (2005).
3. Deleault, N.R., Harris, B.T., Rees, J.R. & Supattapone, S. *Proc. Natl. Acad. Sci. USA* **104**, 9741–9746 (2007).
4. Saborio, G.P., Permanne, B. & Soto, C. *Nature* **411**, 810–813 (2001).
5. Saa, P., Castilla, J. & Soto, C. *J. Biol. Chem.* **281**, 35245–35252 (2006).
6. Atarashi, R. *et al. Nat. Methods* **4**, 645–650 (2007).

GFP fails to inhibit actin-myosin interactions *in vitro*

To the editor: In a Correspondence in *Nature Methods*, Agbulut *et al.*[1] reported dysregulation of calcium excitation-contraction coupling in myoblasts associated with enhanced GFP (eGFP) expression. Additional biochemical analysis led to the conclusion that eGFP directly inhibits the actin-myosin interaction[2]. In contrast, two groups that use a GFP-myosin chimera reported no defects in myosin function[3,4]. Agbulut *et al.* propose that having the GFP tethered to myosin prevents GFP from inhibiting myosin activity in an intramolecular manner[2], but this does not explain why no defects had been seen in solution-based actin-activated ATPase assays, in which intermolecular inhibition might be predicted if eGFP does indeed interact with the actin-binding site of myosin.

Our interest in this topic stems from our work with human muscle myosins II and mutations in them that cause cardiac and skeletal muscle disease. We recently developed a mammalian overexpression system for these myosins using a C-terminal eGFP fusion (manuscript in preparation), and we have not observed any deleterious intra- or intermolecular effects.

To determine whether eGFP might affect the actin-myosin interactions of our chimeras, we repeated many of the experiments conducted by Agbulut *et al.*[1,2], and obtained contradictory results. We performed *in vitro* motility assays with rabbit heavy meromyosin (HMM) and eGFP-6His (**Supplementary Methods** online), and did not observe any significant changes from control assays in the velocity of gliding actin filaments with myosin head/eGFP molar ratios of both 1:1 and 1:10 (**Fig. 1a**). We also obtained similar results with full-length chicken skeletal myosin both when we mixed eGFP with myosin before addition to the motility chamber and when we added eGFP to the motility buffer (data not shown). Even a myosin head/eGFP ratio of over 1:50 yielded no significant reduction in actin-filament velocity (not shown).

We also conducted actin-activated ATPase assays using rabbit HMM and eGFP-6His. The Michaelis-Menten curves (**Fig. 1b**) and derived maximal actin-activated ATPase rates (V_{max}) and Michaelis constants (K_M) (**Supplementary Fig. 1** online) for myosin-head/eGFP ratios ranging from 1:1 to 1:10 did not show any significant differences from control reactions.

We also performed coprecipitation assays to determine whether there is a stable physical interaction between myosin and eGFP. We mixed full-length chicken skeletal muscle myosin and eGFP-6His at a myosin-head/eGFP-6xHis ratio of 1:1, and precipitated this mixture with nickel-agarose beads, using the methodology described by Agbulut *et al.*[2]. We detected no myosin in the elution fraction (**Fig. 1c**), indicating that myosin and eGFP do not coprecipitate. We also performed this experiment in reverse, mixing myosin and eGFP-6His in low-salt buffer, promoting assembly of myosin into insoluble, synthetic thick filaments. Myosin was completely contained in the insoluble fraction, and eGFP-6His was completely contained in the soluble fraction (**Fig. 1d**), confirming that there is no stable interaction between myosin and eGFP. Agbulut *et al.* propose that specific surface electrostatic interactions between eGFP and myosin may stabilize their binding[2], but our coprecipitation assays with nickel-agarose

THE JOURNAL OF BIOLOGICAL CHEMISTRY VOL. 283, NO. 35, pp. 24202–24211, August 29, 2008

Dominant-negative Effects of the N-terminal Half of Prion Protein on Neurotoxicity of Prion Protein-like Protein/Doppel in Mice*

Received for publication, June 2, 2008, and in revised form, June 16, 2008 Published, JBC Papers in Press, June 18, 2008, DOI 10.1074/jbc.M804212200

Daisuke Yoshikawa[‡], Naohiro Yamaguchi[‡], Daisuke Ishibashi[‡], Hitoki Yamanaka[§], Nobuhiko Okimura[‡], Yoshitaka Yamaguchi[¶], Tsuyoshi Mori[¶], Hironori Miyata[‖], Kazuto Shigematsu[**], Shigeru Katamine[‡], and Suehiro Sakaguchi[‡§¶1]

From the [‡]Department of Molecular Microbiology and Immunology, Nagasaki University Graduate School of Biomedical Sciences, 1-12-4 Sakamoto, Nagasaki 852-8523, [§]PRESTO Japan Science and Technology Agency, 4-1-8 Honcho Kawaguchi, Saitama 332-0012, [¶]Division of Molecular Neurobiology, The Institute for Enzyme Research, the University of Tokushima, 3-18-15 Kuramoto-cho, Tokushima 770-8503, [‖]Animal Research Center, University of Occupational and Environmental Health, 1-1 Iseigaoka, Yahatanishi, Kitakyushu 807-8555, and the [**]Department of Pathology, Nagasaki University Graduate School of Biomedical Sciences, 1-12-4 Sakamoto, Nagasaki 852-8523, Japan

Prion protein-like protein/doppel is neurotoxic, causing ataxia and Purkinje cell degeneration in mice, whereas prion protein antagonizes doppel-induced neurodegeneration. Doppel is homologous to the C-terminal half of prion protein but lacks the amino acid sequences corresponding to the N-terminal half of prion protein. We show here that transgenic mice expressing a fusion protein consisting of the N-terminal half, corresponding to residues 1–124, of prion protein and doppel in neurons failed to develop any neurological signs for up to 730 days in a background devoid of prion protein. In addition, the fusion protein prolonged the onset of ataxia in mice expressing exogenous doppel. These results suggested that the N-terminal part of prion protein has a neuroprotective potential acting both *cis* and *trans* on doppel. We also show that prion protein lacking the pre-octapeptide repeat (Δ25–50) or octapeptide repeat (Δ51–90) region alone could not impair the antagonistic function against doppel.

The normal prion protein (PrP^C)[2] is a glycosylphosphatidylinositol (GPI)-anchored membrane glycoprotein expressed most abundantly in the central nervous system, particularly in neurons, and to a lesser extent in non-neuronal tissues, including the heart, lung, spleen, and kidney (1, 2). It is well known that conformational conversion of PrP^C into the abnormally folded amyloidogenic isoform, PrP^{Sc}, plays a pivotal role in the pathogenesis of transmissible spongiform encephalopathies or prion diseases, including Creutzfeldt-Jakob disease in humans and bovine spongiform encephalopathy in cattle (1, 3). However, the physiological function of PrP^C remains largely unknown.

We and others identified a novel gene, *Prnd*, that encodes a GPI-anchored PrP-like protein, termed Doppel (Dpl), 16 kb downstream of the murine PrP gene *Prnp* (4, 5). Dpl is expressed in the testis, heart, kidney, and spleen of wild-type mice but not in the brain where PrP^C is actively expressed. Intriguingly, some lines of mice devoid of PrP^C ($Prnp^{0/0}$), including Ngsk, Rcm0, and Zrch II, ectopically expressed Dpl in their brains, particularly in neurons, because of an unusual intergenic splicing between *Prnp* and *Prnd*, developed ataxia, and Purkinje cell degeneration (5, 6). However, others, such as Zrch I and Npu, neither ectopically expressed Dpl nor exhibited ataxia and Purkinje cell degeneration (4, 5). It was finally confirmed that Dpl is neurotoxic, and PrP^C antagonizes the neurotoxicity of Dpl by a demonstration that transgenically expressed Dpl caused ataxia and Purkinje cell degeneration in nonataxic Zrch I $Prnp^{0/0}$ mice but not in wild-type mice (7–9). However, the exact mechanism of the antagonistic interaction of PrP^C and Dpl remains unknown.

Dpl shares 23% identity in amino acid composition with PrP (4, 5) and bears conformational similarity to the C-terminal globular domain of PrP^C, both comprising three α-strands and two short β-strands (10). However, Dpl lacks the amino acid sequences corresponding to the N-terminal half of PrP^C (4, 5). Interestingly, it was shown that PrP with truncated N-terminal residues 32–121 or 32–134, termed PrPΔ32–121 or PrPΔ32–134, respectively, exhibited neurotoxicity similarly to that of Dpl, causing ataxia and cerebellar neurodegeneration in nonataxic Zrch I $Prnp^{0/0}$ mice but not in wild-type mice (11, 12). Therefore, it might be possible that the neurotoxicity of Dpl is attributable to lack of the corresponding N-terminal part of PrP^C. However, this remains to be elucidated.

We previously showed that the N-terminal residues 23–88 of PrP^C are involved in the antagonistic function of PrP^C against the Dpl neurotoxicity by demonstrating that PrP lacking the residues 23–88 completely lost the ability to rescue Ngsk $Prnp^{0/0}$ mice from Dpl-induced Purkinje cell degeneration (13). Residues 23–88 include most of the PrP-specific octapeptide

* This study was supported in part by a Research on Specific Diseases grant from the Ministry of Health, Labor and Welfare, Japan. The costs of publication of this article were defrayed in part by the payment of page charges. This article must therefore be hereby marked "*advertisement*" in accordance with 18 U.S.C. Section 1734 solely to indicate this fact.

[1] To whom correspondence should be addressed: Division of Molecular Cytology, Institute for Enzyme Research, University of Tokushima, 3-18-15 Kuramoto-cho, Tokushima 770-8503, Japan. Tel.: 81-88-633-7438; Fax: 81-88-633-7440; E-mail: sakaguch@ier.tokushima-u.ac.jp.

[2] The abbreviations used are: PrP, prion protein; Dpl, doppel; OR, octapeptide repeat; GPI, glycosylphosphatidylinositol; tg, transgenic; dtg, double transgenic; SOD, superoxide dismutase; PNGase, peptide:*N*-glycosidase.

repeat (OR) region, which includes residues 51–90. Recent lines of evidence from cell culture experiments show that the OR may be involved in the neuroprotective function of PrP^{C} (14–16). However, the biological relevance of OR in the neuroprotective function of PrP^{C} against Dpl is not yet understood *in vivo*.

In this study, we generated transgenic (tg) mice, tg(PrPΔOR) and tg(PrPN-Dpl), expressing PrP lacking OR and Dpl fused with the N-terminal half of PrP^{C}, respectively. We also produced tg(PrPΔpreOR) mice expressing PrP without the pre-OR region. By intercrossing these tg mice with mice transgenically overexpressing Dpl in neurons on the genetic background of nonataxic Zrch I $Prnp^{0/0}$, we investigated whether or not these mutant molecules could antagonize Dpl neurotoxicity, rescuing mice from ataxia and Purkinje cell degeneration.

EXPERIMENTAL PROCEDURES

Construction of Transgenes—A DNA fragment corresponding to the N-terminal residues 1–124 of PrP was first amplified by PCR with primer a (5′-cccaagcttctcgag**atg**gcgaaccttggc-3′, the underlined sequence corresponds to the HindIII and XhoI sites, and the boldface sequence represents a start codon) and primer f (5′-cttgatgaaggctcc*aaggccccccactac*-3′, the underlined sequence corresponds to DNA encompassing residues 58–62 of Dpl, and the italic sequence corresponds to DNA encompassing residues 120–124 of PrP) using PrP cDNA as a template. The resulting DNA fragment, containing the DNA sequence corresponding to residues 58–62 of Dpl at the 3′ site, was then utilized as a 5′ primer to amplify another DNA fragment corresponding to residues 58–179 of Dpl together with primer i (5′-cccaagcttctcgag**tta**cttcacaatgaa-3′, the underlined sequence corresponds to the HindIII and XhoI sites, and the boldface sequence represents a stop codon) using Dpl cDNA as a template, resulting in amplification of a DNA fragment for the fusion protein PrPN-Dpl consisting of residues 1–124 of PrP and residues 58–179 of Dpl. After DNA sequence confirmation of the amplified fragment, it was inserted into a unique SalI site of the Syrian hamster PrP cosmid vector, CosSHa.tet (InPro Biotechnology, Inc. South San Francisco, CA), to construct the PrPN-Dpl transgene.

A DNA fragment corresponding to the N-terminal residues 1–24 of PrP was first amplified by PCR with primers a and c (5′-ggtgccaccctgaggc*tttttgcagaggcc*-3′, the underlined and italic sequences correspond to DNAs encompassing residues 51–55 and 20–24 of PrP, respectively) using PrP cDNA as a template. The resulting DNA fragment containing the DNA sequence corresponding to residues 51–55 of PrP at the 3′ site was then utilized as a 5′ primer to amplify another DNA fragment corresponding to residues 51–254 of PrP together with primer g (5′-cccaagcttctcgag**tca**tcccacgatcag-3′, the underlined sequence corresponds to the HindIII and XhoI sites, and the boldface sequence represents a stop codon) using PrP cDNA as a template, resulting in amplification of a DNA fragment for the deletion protein PrPΔpreOR consisting of residues 1–24 and 51–254 of PrP. After DNA sequence confirmation of the amplified fragment, it was inserted into a unique SalI site of the Syrian hamster PrP cosmid vector, CosSHa.tet (InPro Biotechnology, Inc.), to construct the PrPΔpreOR transgene.

A DNA fragment corresponding to the N-terminal residues 1–50 of PrP was first amplified by PCR with primers a and d (5′-atgggtacccccctcc*tgggtaacggttgcc*-3′, the underlined and italic sequences correspond to DNAs encompassing residues 91–95 and 46–50 of PrP, respectively) using PrP cDNA as a template. The resulting DNA fragment containing the DNA sequence corresponding to residues 91–95 of PrP at the 3′ site was then utilized as a 5′ primer to amplify another DNA fragment corresponding to residues 91–254 of PrP together with primer g using PrP cDNA as a template, resulting in amplification of a DNA fragment for the deletion protein PrPΔOR consisting of residues 1–50 and 91–254 of PrP. After DNA sequence confirmation of the amplified fragment, it was inserted into a unique SalI site of the Syrian hamster PrP cosmid vector, CosSHa.tet (InPro Biotechnology, Inc.), to construct the PrPΔOR transgene.

Generation of Transgenic Mice—The plasmid-derived sequences were removed from each of the transgene constructs, and the resulting DNAs were injected into the zygotes of C57BL/6 mice to generate tg mice as described elsewhere (17, 18).

Expression Vectors for Wild-type PrP^{C}, PrPΔpreOR, PrPΔOR, and PrPΔ23–88—The DNA fragments encoding wild-type mouse PrP^{C} and PrPΔ23–88 were amplified by PCR with a sense primer (5′-tcggatccagtcatc**atg**gcgaaccttggc-3′; the underlined sequence corresponds to a BamHI site; the boldface sequence corresponds to a start codon) and an antisense primer (5′-cctctagac**tca**tcccacgatcaggaaga-3′; the underlined sequence corresponds to an XbaI site; the boldface sequence corresponds to a stop codon) using mouse genomic DNA extracted from wild-type mice and tg(PrPΔ23–88) mice (13). After confirmation of the DNA sequences, each DNA fragment was digested by BamHI and XbaI and introduced into a pcDNA3.1 vector (Invitrogen) to generate pcDNA3.1-moPrP and pcDNA3.1-PrPΔ23–88. pcDNA3.1-PrPΔpreOR and -PrPΔOR were constructed by digestion of each of the already cloned PCR products with HindIII and subsequent insertion of the digested fragments into a HindIII site of pcDNA3.1 vector.

Breeding Procedures—Zrch I $Prnp^{0/0}$ mice on the C57BL/6 × 129Sv mixed background and tg(Dpl32) mice on the C57BL/6 background were generated as described (8, 19). tg(Dpl32)/$Prnp^{0/0}$ mice were previously produced by serially mating tg(Dpl32) mice (C57BL/6) with Zrch I $Prnp^{0/0}$ mice, which were obtained by mating pairs of Zrch I $Prnp^{+/0}$ mice that had been generated by crossing Zrch I $Prnp^{0/0}$ mice (C57BL/6 × 129Sv) with FVB wild-type mice. Thus, tg(Dpl32)/$Prnp^{0/0}$ mice have a mixed genetic background of C57BL/6 × 129Sv × FVB. Tg(PrPN-Dpl), tg(PrPΔpreOR), and tg(PrPΔOR) mice were successively mated with Zrch I $Prnp^{0/0}$ mice, which had been backcrossed with C57BL/6 mice at least nine times, to produce each line of tg mice with the Zrch I $Prnp^{0/0}$ genetic background. The resulting tg mice with the Zrch I $Prnp^{0/0}$ genetic background were then mated with tg(Dpl)/$Prnp^{0/0}$ mice (C57BL/6 × 129Sv × FVB) to produce each line of double tg (dtg) mice co-expressing each of the respective transgenes and Dpl on the Zrch I $Prnp^{0/0}$ genetic background. Therefore, all dtg mice have a mixed genetic background of C57BL/6 × 129Sv × FVB. Ani-

mals were cared for in accordance with the Guidelines for Animal Experimentation of Nagasaki University.

Diagnosis of Ataxia—The behavior of mice was inspected at least every 3 days evaluating difficulties for walking straight or trembling in their hindquarters on initiation of movement and during walking. When mice showed such abnormal behaviors, they were subjected to a second inspection at least 3 days later. At this time, if the same or exacerbated symptoms were obvious, mice were diagnosed with ataxia, and the date of the first recognition of the abnormal behaviors was registered as the onset of the ataxia. If the symptoms were trivial or difficult to diagnose as ataxia by an investigator, another investigator also inspected the mice to confirm the symptoms. In this case, mice were not diagnosed as ataxia until the two investigators independently confirmed the symptoms.

Western Blotting—Homogenates (10%, w/v) were prepared in a lysis buffer containing 150 mM NaCl, 50 mM Tris-HCl, pH 7.5, 0.5% Triton X-100, 0.5% sodium deoxycholate, 1 mM EDTA, and protease inhibitor mixture (Nakalai Tesque Co., Kyoto, Japan) and centrifuged at low speed. Protein concentrations of the resulting supernatant were determined using the BCA protein assay kit (Pierce). Total proteins were electrophoresed through a 12% SDS-polyacrylamide gel and electrically transferred to an Immobilon-P polyvinylidene difluoride membrane (Millipore Corp.). The membrane was immersed in 5% nonfat dry milk containing TBST (0.1% Tween 20, 100 mM NaCl, 10 mM Tris-HCl, pH 7.6) for 1 h at room temperature and incubated with M20 goat polyclonal antibodies (Santa Cruz Biotechnology, Santa Cruz, CA), SAF32 mouse monoclonal antibody (SPI-BIO, Montigny le Bretonneux, France), or FL176 rabbit polyclonal antibodies against human Dpl (Santa Cruz Biotechnology) for 2 h at room temperature in 1% nonfat dry milk containing TBST. The membrane was washed once in TBST for 15 min and three times for 5 min. Signals were visualized using horseradish peroxidase-conjugated secondary antibodies (Amersham Biosciences) and the ECL system (Amersham Biosciences).

PNGase F Digestion—PNGase F digestion was performed according to the manufacturer's protocol (New England Biolabs, Inc., Ipswich, MA). Briefly, mouse brain homogenates were denatured by boiling for 10 min in the presence of 0.5% SDS and 1% mercaptoethanol and then treated with PNGase F (500 units/liter) in 1% Nonidet P-40 and 0.05 M sodium phosphate, pH 7.5, for 60 min at 37 °C.

In Situ Hybridization—*In situ* hybridization was performed as described elsewhere (8). Briefly, mouse brains were fixed in 4% paraformaldehyde, embedded in paraffin, and sliced to 5 μm thickness. The tissue sections were then deparaffinized, digested with 10 mg/ml proteinase K for 10 min at 37 °C, and soaked in 0.25% acetic anhydride, 0.1 mM triethanolamine hydrochloride, pH 8.0, 0.9% NaCl for 10 min. After this, the sections were hybridized with PrP cRNA probes labeled with digoxigenin-UTP (Roche Diagnostics) in buffer (50% formamide, 10 mM Tris-HCl, pH 7.5, 1 mM EDTA, 0.6 M NaCl, 0.5 mg/ml yeast tRNA, 0.25% SDS, 5× Denhardt's solution) at 50 °C for 16 h, and followed by several washes in 4× SSC and immersion in 50% formamide, 2× SSC at 50 °C for 30 min. The probe used for PrP was derived from the PCR product corresponding to PrP residues 26–187. The hybridized sections were then digested with 20 μg/ml RNase A at 37 °C for 30 min and finally washed in 0.2× SSC at 50 °C for 20 min. Signals were detected by enzyme-linked immunosorbent assay using alkaline phosphatase-conjugated anti-digoxigenin Fab fragments (1:500, Roche Diagnostics) and nitro blue tetrazolium/5-bromo-4-chloro-3-indolyl phosphate.

Immunohistochemistry—Deparaffinized sections were placed in 3% H_2O_2 in methanol for 30 min at room temperature to abolish endogenous peroxidase activity. The tissue sections were incubated overnight at 4 °C with anti-spot 35 (calbindin) polyclonal antibodies, IBL-N rabbit antibodies against the N-terminal peptide of PrP (Immuno Biological Laboratories, Gunma, Japan), and ICSM-18 monoclonal antibody recognizing residues 146–159 of murine PrP. To detect immunoreactivities, we used the EnVision+ system in accordance with the manufacturer's recommendations (Dako, Glostrup, Denmark). The antibody-bound peroxidase was detected with 0.04% diaminobenzidine (Sigma).

Flow Cytometry—African green monkey kidney COS-7 cells were transiently transfected by pcDNA3.1 vector alone, pcDNA3.1-moPrP, pcDNA3.1-PrPΔpreOR, pcDNA3.1-PrPΔOR, and pcDNA3.1-PrPΔ23–88 using Lipofectamine 2000 (Invitrogen). The cells were harvested with phosphate-buffered saline containing 20 mM EDTA 48 h after transfection, suspended in 5% fetal bovine serum-containing BSS buffer (140 mM NaCl, 5.4 mM KCl, 0.8 mM $MgSO_4$, 0.3 mM Na_2HPO_4, 0.4 mM KH_2PO_4, 1 mM $CaCl_2$, pH 7.0), and incubated with 100-fold diluted SAF61 antibodies for 1 h on ice. The treated cells were then washed twice with 5% fetal bovine serum-containing BSS buffer, incubated with Alexa Fluor 488 goat anti-mouse IgG (H+L) (Invitrogen), and analyzed by EPICS XL (Beckman Coulter Inc., Fullerton, CA).

RESULTS

Generation and Characterization of tg(PrPN-Dpl), tg(PrPΔpreOR), and tg(PrPΔOR) Mice—The amino acid alignment of PrP and Dpl depicts the homology between the C-terminal regions of the two proteins, corresponding to the residues 125–254 of PrP and 58–179 of Dpl, both of which form a neurotoxic globular structure with three α-helices and two β-strands (Fig. 1*A*). Therefore, to evaluate the effects of the N-terminal region of PrP on Dpl in *cis*, the PrP N-terminal residues 1–124 were fused to the Dpl residues 58–179 to make the PrPN-Dpl transgene (Fig. 1*A*). The PrPΔpreOR and PrPΔOR, PrP deletion mutants lacking the N-terminal residues 25–50 and 51–90, respectively, were also constructed to examine the involvement of each region in protection from the Dpl-induced neurodegeneration (Fig. 1*A*). We introduced each corresponding DNA into the Syrian hamster PrP cosmid vector, CosSHa.tet (20), allowing each of the mutant proteins to be expressed under the control of the hamster PrP promoter (Fig. 1*B*). These transgenes were then microinjected into fertilized eggs of C57BL/6 mice, yielding four founders from the PrPN-Dpl transgene and two from each of the PrPΔpreOR and PrPΔOR transgenes. All of these founders successfully transferred the transgenes into their offspring. These tg mice were successively intercrossed with nonataxic Zrch I $Prnp^{0/0}$ mice to eliminate endogenous PrP^C.

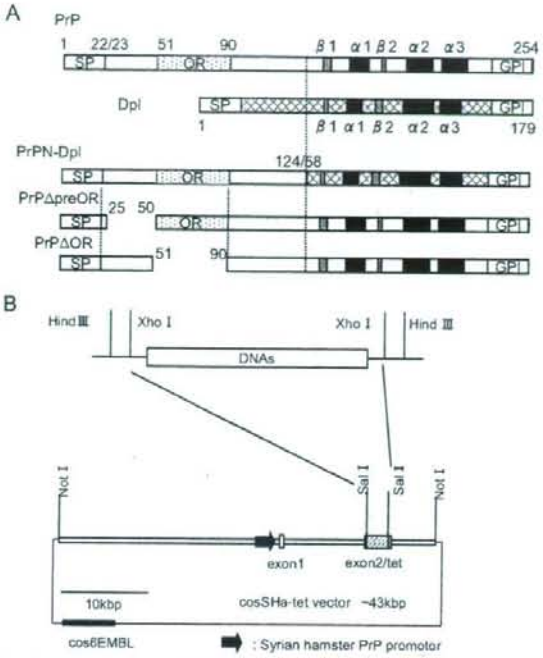

FIGURE 1. *A*, schematic representations of the mutant proteins, PrPN-Dpl, PrPΔpreOR, and PrPΔOR. PrPN-Dpl is a fusion protein consisting of the N-terminal residues 1–124 of PrP and the residues 58–179 of Dpl. PrPΔpreOR and PrPΔOR lack the residues 25–50 (*preOR*) and 51–90 (*OR*) of PrP, respectively. *Arabic numbers* represent the codon numbers. *SP*, signal peptide; *OR*, octapeptide repeat; *GPI*, GPI anchor signal; α, α-helix; β, β-strand. *B*, configuration of the transgenes. Each transgene was constructed by replacing the DNA fragment encoding PrPN-Dpl, PrPΔpreOR, or PrPΔOR with a Sal-Sal fragment of the cosSHa-tet vector carrying the Syrian hamster PrP promoter. The vector-derived DNAs were removed by digestion with NotI, and the purified fragments were used as transgenes.

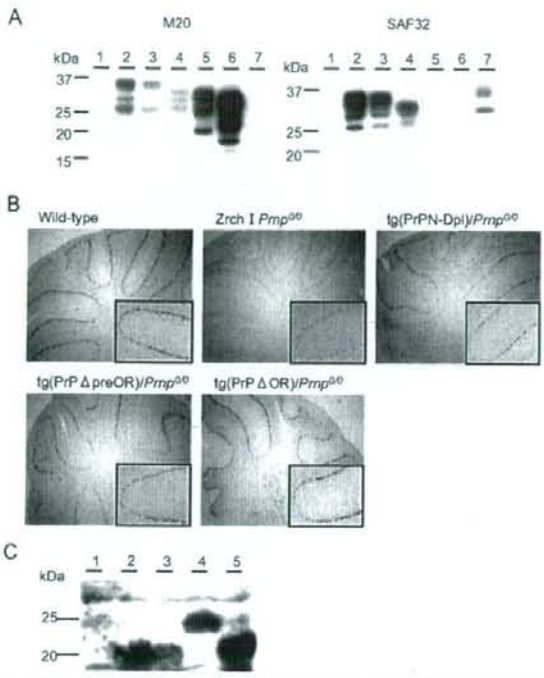

FIGURE 2. *A*, Western blotting of the cerebella of tg(PrPN-Dpl)/$Prnp^{0/0}$, tg(PrPΔpreOR)/$Prnp^{0/0}$, and tg(PrPΔOR)/$Prnp^{0/0}$ mice. 30 μg of the total proteins were loaded onto each lane. *Lane 1*, Zrch I $Prnp^{0/0}$ mice; *lane 2*, wild-type mice; *lane 3*, Zrch I $Prnp^{0/+}$ mice; *lane 4*, tg(PrPΔpreOR)/$Prnp^{0/0}$ mice; *lane 5*, tg(PrPΔOR)/$Prnp^{0/0}$ mice; *lane 6*, tg(MHM2Δ23–88)/$Prnp^{0/0}$ mice; *lane 7*, tg(PrPN-Dpl)/$Prnp^{0/0}$ mice. *B*, *in situ* hybridization of the cerebella of wild-type, Zrch I $Prnp^{0/0}$, tg(PrPN-Dpl)/$Prnp^{0/0}$, tg(PrPΔpreOR)/$Prnp^{0/0}$, and tg(PrPΔOR)/$Prnp^{0/0}$ mice. Purkinje cells in Zrch I $Prnp^{0/0}$ mice show background staining with the PrP cRNA probe. In contrast, strongly stained Purkinje cells are observed in wild-type, tg(PrPN-Dpl)/$Prnp^{0/0}$, tg(PrPΔpreOR)/$Prnp^{0/0}$, and tg(PrPΔOR)/$Prnp^{0/0}$ mice. Magnification, ×10; *inset* magnification, ×50. *C*, Western blotting of the PNGase F-treated homogenates of the cerebella from wild-type (*lane 1*, 100 μg of the total proteins), Ngsk $Prnp^{0/0}$ (*lane 2*, 100 μg), Ngsk $Prnp^{0/+}$ (*lane 3*, 100 μg), tg(PrPN-Dpl)/$Prnp^{0/0}$ (*lane 4*, 200 μg), and tg(Dpl32)/$Prnp^{0/0}$ mice (*lane 5*, 100 μg) using anti-Dpl FL176 antibodies.

The expression of mutant proteins was confirmed in 1/2 tg(PrPΔpreOR)/$Prnp^{0/0}$, 2/2 tg(PrPΔOR)/$Prnp^{0/0}$, and 1/4 tg(PrPN-Dpl)/$Prnp^{0/0}$ mice by Western blotting. As shown in Fig. 2*A*, goat M-20 antibodies against the C-terminal PrP peptide visualized bands in the cerebellar tissue homogenates from tg(PrPΔpreOR)/$Prnp^{0/0}$ and tg(PrPΔOR)/$Prnp^{0/0}$ mice (*left panel, lanes 4* and *5*). These bands migrated slightly faster than authentic PrP^C of wild-type mice. But M20 antibodies did not detect any immunoreactivities in tg(PrPN-Dpl) mice (Fig. 2*A*, *lane 7*). On the other hand, SAF32 anti-OR antibodies revealed signals in the cerebellum of tg(PrPΔpreOR)/$Prnp^{0/0}$ and tg(PrPN-Dpl)/$Prnp^{0/0}$ mice, but not in tg(PrPΔOR)/$Prnp^{0/0}$ mice (Fig. 2*A*, *right panel*). *In situ* hybridization showed that each transgene was ubiquitously expressed over the brain, with the strongest signals being detectable in Purkinje cells (Fig. 2*B*) and hippocampal neurons (data not shown). In Zrch I $Prnp^{0/0}$ mice, some Purkinje cells were faintly stained because of nonspecific hybridization of the probe because no PrP could be detected by Western blotting (Fig. 2, *A*, *lane 1*, and *B*).

We also performed immunohistochemical analysis of cerebella from these tg mice with the Zrch I $Prnp^{0/0}$ background using two different antibodies, rabbit polyclonal IBL-N and mouse monoclonal ICSM-18 antibodies, which are directed against residues 24–37 and 146–159 of murine PrP, respectively. Both antibodies showed no immunoreactivities in the cerebella of Zrch I $Prnp^{0/0}$ mice (Fig. 3, *E–H*). In contrast, the molecular and granule cell layers of normal C57BL/6 mice were clearly stained with both antibodies (Fig. 3, *A–D*). However, there seemed to be no immunoreactivity in the Purkinje cell layer (Fig. 3, *A–D*). These staining patterns of PrP^C in the cerebellum of normal mice were consistent with previous reports (21–23). PrPΔpreOR mutant protein was expressed in the cerebella of tg(PrPΔpreOR)/$Prnp^{0/0}$ mice indistinguishably from PrP^C in C57BL/6 mice, detectable in the molecular and granule cell layers but not in the Purkinje cell layer (Fig. 3, *K* and *L*). PrPΔOR and PrPN-Dpl mutant proteins were also expressed in the molecular and granule cell layers of tg(PrPΔOR)/$Prnp^{0/0}$ and tg(PrPN-Dpl)/$Prnp^{0/0}$ mice, respectively (Fig. 3, *M–R*). However, the mutant proteins were more abundant in the granule cell layer than in the molecular layer (Fig. 3, *M–R*). Moreover, in tg(PrPΔOR)/$Prnp^{0/0}$ mice, the Purkinje cell layer was

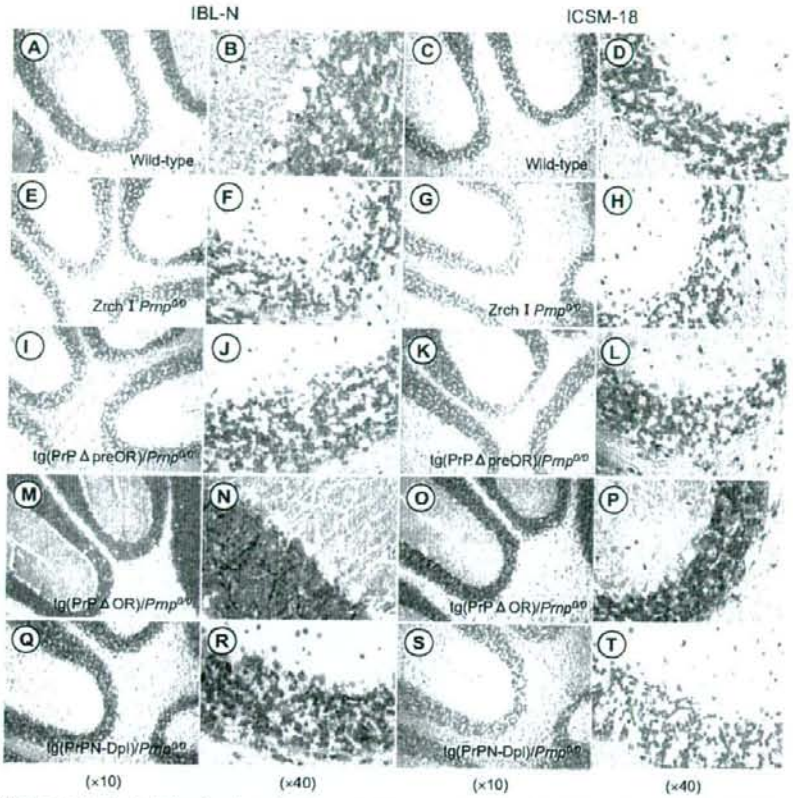

FIGURE 3. **Cytological distribution of PrPΔpreOR, PrPΔOR, and PrPN-Dpl in the cerebella of tg mice.** The cerebellar sections from CS7BL/6 (*A–D*), Zrch I $Prnp^{0/0}$ mice (*E–H*), tg(PrPΔpreOR)/$Prnp^{0/0}$ mice (*I–L*), tg(PrPΔOR)/$Prnp^{0/0}$ mice (*M–P*), and tg(PrPN-Dpl)/$Prnp^{0/0}$ mice (*Q–T*) were subjected to immunohistochemistry using IBL-N and ICSM-18 antibodies, which are directed against PrP residues 24–37 and 146–159, respectively.

devoid of the signal, but the basolateral area surrounding some but not all Purkinje cells was strongly stained (Fig. 3, *M* and *N* and Fig. 7). In tg(PrPN-Dpl)/$Prnp^{0/0}$ mice, the cell bodies of Purkinje cells appeared positive, and some cells scattered in the granule cell layer were strongly stained in the cell bodies (Fig. 3, *Q* and *R*). These cells are currently unidentified. Moreover, cortical neurons of tg(PrPN-Dpl)/$Prnp^{0/0}$ mice but not wild-type and tg(PrPΔOR)/$Prnp^{0/0}$ mice were positively stained in the cell bodies by IBL-N antibodies (data not shown).

PrPN-Dpl Delays Onset of Dpl-induced Ataxia and Purkinje Cell Degeneration in Mice—No tg(PrPN-Dpl)/$Prnp^{0/0}$ mice showed any abnormal symptoms, including ataxia, up to 730 days after birth, at the time of writing (Fig. 4*A*). Purkinje cells were also unaffected in these mice (data not shown). The signals visualized by anti-Dpl antibodies on a Western blot of brain homogenates from tg mice was about 35% that of Ngsk $Prnp^{0/0}$ mice, ectopically expressing Dpl in neurons under the control of the PrP promoter (Fig. 2*C*). These results indicate that, unlike wild-type Dpl, the fusion protein PrPN-Dpl might be nontoxic to Purkinje cells even in the absence of PrP^C, although we could not completely rule out the possibility that the lack of neurotoxicity of PrPN-Dpl is because of its lower expression.

We next generated dtg mice by intercrossing tg(PrPN-Dpl)/$Prnp^{0/0}$ mice with tg(Dpl32)/$Prnp^{0/0}$ mice, expressing the full-length Dpl in neurons, including Purkinje cells under the control of the neuron-specific enolase promoter at a level higher than that in Ngsk $Prnp^{0/0}$ mice (Fig. 2*C*), which develop ataxia because of Purkinje cell degeneration 99 ± 20 days after birth (Fig. 4*A*, Table 1, and Fig. 5). The times of onset of ataxia in tg(Dpl32)/$Prnp^{0/0}$ mice were slightly prolonged compared with those reported previously (8). This is probably because we employed more strict criteria for diagnosis of ataxia in this study. The resulting dtg(PrPN-Dpl)(Dpl32)/$Prnp^{0/0}$ mice eventually suffered from ataxia, but their onsets were significantly delayed to 200 ± 52 days after birth (Fig. 4*A* and Table 1). Consistent with this, immunohistochemistry using antibodies against calbindin, a Purkinje cell-specific marker, revealed well preserved Purkinje cells in the dtg mice 90 days after birth (Fig. 5), when Purkinje cells had been significantly lost in tg(Dpl32)/$Prnp^{0/0}$ mice (Fig. 5). No decreased expression of Dpl could be detected in the brains of dtg(PrPN-Dpl)(Dpl32)/$Prnp^{0/0}$ mice, compared with tg(Dpl32)/$Prnp^{0/0}$ mice (Fig. 6). These results indicate that the fusion protein PrPN-Dpl antagonizes the Dpl-induced neurotoxicity, similar to PrP^C.

PrPΔpreOR and PrPΔOR Inhibit Dpl-induced Ataxia and Purkinje Cell Degeneration in Mice—To evaluate the potential of PrPΔpreOR and PrPΔOR to antagonize the neurotoxicity of Dpl, tg(PrPΔpreOR)/$Prnp^{0/0}$ and tg(PrPΔOR)/$Prnp^{0/0}$ mice were intercrossed with tg(Dpl32)/$Prnp^{0/0}$ mice. We previously showed that the onset of ataxia by Dpl-induced Purkinje cell degeneration depended on the expression levels of wild-type PrP^C, and neither ataxia nor Purkinje cell degeneration occurred in tg(Dpl32) mice on the wild-type ($Prnp^{+/+}$) background (8). The expression levels of PrPΔOR and PrPΔpreOR in each of the dtg mouse lines, dtg(PrPΔOR)(Dpl32)/$Prnp^{0/0}$ and dtg(PrPΔpreOR)(Dpl32)/$Prnp^{0/0}$, were 1.7- and 0.4-fold, respectively, of the level of PrP^C in wild-type mice (Fig. 2*A*). The dtg(PrPΔOR)(Dpl32)/$Prnp^{0/0}$ mice showed no ataxic symptoms up to 500 days after birth (Fig. 4*B* and Table 1). On the other hand, dtg(PrPΔpreOR)(Dpl32)/$Prnp^{0/0}$ mice developed ataxia 385 ± 47 days after birth, which was very delayed compared with the onset in tg(Dpl32)/$Prnp^{0/0}$ mice (99 ± 20 days)

and similar to that in tg(Dpl32) mice on the heterozygous *Prnp* background ($Prnp^{+/0}$), 387 ± 25 days (Fig. 4*B* and Table 1). In contrast to tg(Dpl32)/$Prnp^{0/0}$, Purkinje cells were unaffected in both dtg mouse lines 90 days after birth on the PrP-null background (Fig. 5). Moreover, Dpl was not decreased in the brains of these dtg mice, compared with tg(Dpl32) mice (Fig. 6). These results indicate that PrPΔpreOR and PrPΔOR preserve the potential to protect from Dpl-induced Purkinje cell degeneration.

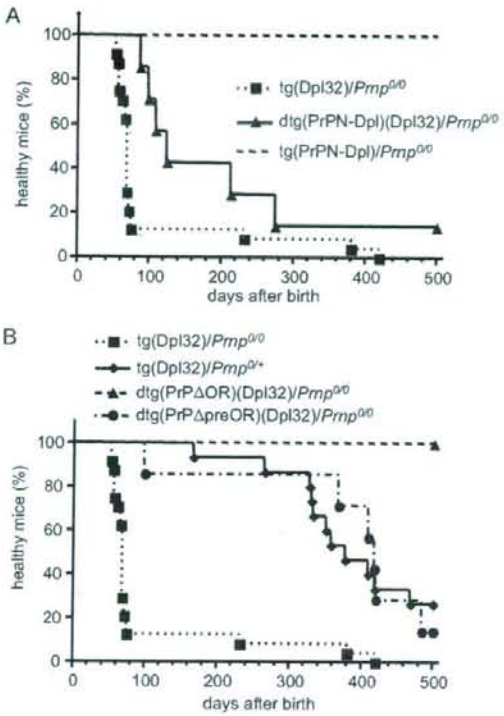

FIGURE 4. *A*, rescue from ataxia in dtg(PrPN-Dpl)(Dpl32)/$Prnp^{0/0}$ mice. No ataxic symptoms were observed in tg(PrPN-Dpl)/$Prnp^{0/0}$ mice for up to at least 500 days after birth. In contrast, tg(Dpl32)/$Prnp^{0/0}$ mice developed ataxia 99 ± 20 days after birth. The PrPN-Dpl transgene delayed the onset of ataxia in tg(Dpl32) mice to 200 ± 52 days, as observed in dtg(PrPN-Dpl)(Dpl32)/$Prnp^{0/0}$ mice. *B*, rescue of the ataxia in dtg(PrPΔpreOR)(Dpl32)/$Prnp^{0/0}$ and dtg(PrPΔOR)(Dpl32)/$Prnp^{0/0}$ mice. No ataxic symptoms were observed in dtg(PrPΔOR)(Dpl32)/$Prnp^{0/0}$ mice for up to at least 500 days after birth. dtg(PrPΔpreOR)(Dpl32)/$Prnp^{0/0}$ mice developed delayed onset of ataxia at 385 ± 47 days after birth similarly to tg(Dpl32)/$Prnp^{0/+}$ mice, those developing ataxia at 387 ± 25 days after birth.

PrPΔ23–88 Is Expressed in the Cerebellum of Mice and on the Surface of Cultured Cells Similarly to Wild-type PrP^C—We previously showed that PrPΔ23–88 was incompetent to rescue Ngsk $Prnp^{0/0}$ mice from the Dpl-induced Purkinje cell degeneration, indicating that the region comprising the residues 23–88 is important for PrP^C to be protective against Dpl (13). To further gain insights into the role of the residues 23–88 in the neuroprotective function of PrP^C, we investigated cytological expression of PrPΔ23–88 in the cerebellum of mice. The cerebella from tg(PrPΔ23–88) mice on the Ngsk $Prnp^{0/0}$ background as well as from Zrch I $Prnp^{0/0}$ and tg(PrPΔOR)/$Prnp^{0/0}$ mice were subjected to immunohistochemistry using IBL-N and ICSM-18 antibodies. Consistent with the results shown in Fig. 3, no signals could be detected in Zrch I $Prnp^{0/0}$ mice, and tg(PrPΔOR)/$Prnp^{0/0}$ mice showed abundant expression of PrPΔOR in the molecular and granule cells layers but not in the Purkinje cell layer (Fig. 7). PrPΔ23–88 was detected in the molecular and granule cell layers but not in the Purkinje cell layer (Fig. 7), similarly to PrPΔOR (Fig. 7) and wild-type PrP^C (Fig. 3, *A–D*). We also investigated the cell surface expression of PrPΔ23–88 using cultured cells in comparison with that of wild-type PrP^C and two other neuroprotective mutants, PrPΔpreOR and PrPΔOR. COS-7 monkey kidney cells were transiently transfected with each expression vector and then subjected to flow cytometry analysis using SAF61 monoclonal antibodies against PrP-(142–160) residues. PrPΔ23–88 was detected on the cell surface of COS-7 cells similarly to that of wild-type PrP^C, PrPΔpreOR, and PrPΔOR (Fig. 8). These results indicate that lack of the residues 23–88 neither alter cell types for PrPΔ23–88 to be expressed in the cerebellum of mice nor impair the cell surface expression of PrPΔ23–88.

DISCUSSION

Accumulating evidence indicates a neuroprotective role for PrP^C. For instance, $Prnp^{0/0}$ mice are highly sensitive to ischemic or traumatic brain damage, developing more severe pathological changes than in wild-type mice (24–27). In contrast, Dpl, the first identified structural homologue of the C-terminal domain of PrP^C, is neurotoxic causing ataxia and Purkinje cell degeneration in mice (7–9). Interestingly, PrP^C functionally antagonizes the neurotoxicity of Dpl, preventing the neurode-

TABLE 1
Antagonistic effects of mutant proteins on Dpl-induced neurotoxicity in tg mice

tg or dtg lines	PrP genetic background	Expression level of mutant or wild-type forms of PrP[a] (fold)	No. of ataxic mice/ No. of total mice	Times to the onset of ataxia[b] (days)	*p* value log rank test
tg(Dpl32)	Zrch I $Prnp^{0/0}$	0	24/24[c]	99 ± 20[d]	
	Zrch I $Prnp^{0/+}$	0.5	11/15[e]	387 ± 25[d]	<0.0001
dtg(PrPN-Dpl)(Dpl32)	Zrch I $Prnp^{0/0}$	0.21	6/7	200 ± 52	0.016
tg(PrPN-Dpl)			0/7	>730	<0.0001
dtg(PrPΔpreOR)(Dpl32)	Zrch I $Prnp^{0/0}$	0.42	6/7	385 ± 47	0.0004
tg(PrPΔpreOR)			0/9	>500	<0.0001
dtg(PrPΔOR)(Dpl32)	Zrch I $Prnp^{0/0}$	1.7	0/6	>500	<0.0001
tg(PrPΔOR)			0/6	>500	<0.0001

[a] Expression levels were compared with those of PrP in wild-type mice using Western blotting.
[b] The times were expressed as mean ± S.E. days after birth.
[c] These 24 mice were produced by breeding of tg(Dpl32)/$Prnp^{0/0}$ mice with tg(PrPN-Dpl)/$Prnp^{0/0}$ mice, tg(PrPΔpreOR)/$Prnp^{0/0}$ mice, and tg(PrPΔOR)/$Prnp^{0/0}$ mice.
[d] These times were slightly different from those previously reported (8) probably due to more strict diagnostic criteria for ataxia.
[e] These 15 mice were produced by breeding tg(Dpl32) mice with Zrch I $Prnp^{0/0}$ mice.

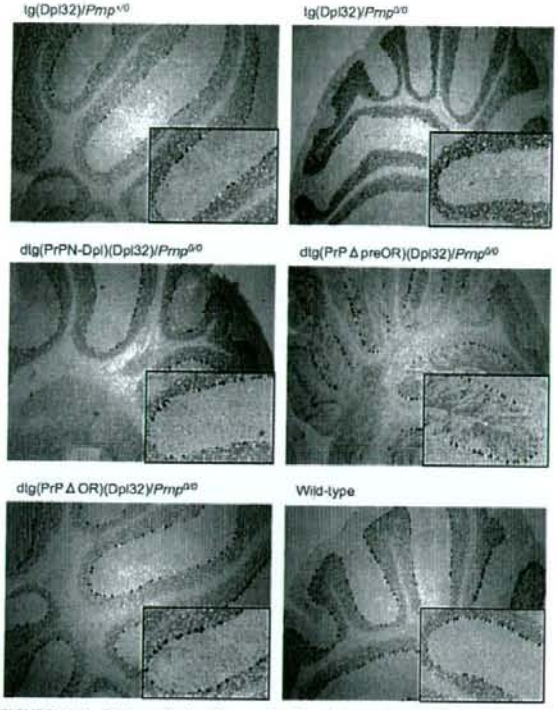

FIGURE 5. **Purkinje cells in the cerebella of dtg mice.** Purkinje cells were immunohistochemically stained using anti-calbindin antibodies and the EnVision+ system. Magnification, ×20; *inset* magnification, ×100.

FIGURE 6. **Western blotting of the PNGase F-treated homogenates (75 μg of total proteins) of the cerebella from Zrch I *Prnp*$^{0/0}$, tg(Dpl32)/*Prnp*$^{0/0}$, tg(Dpl32)/*Prnp*$^{+/0}$, dtg(PrPΔpreOR)(Dpl32)/*Prnp*$^{0/0}$, dtg(PrPΔOR)(Dpl32)/*Prnp*$^{0/0}$, and dtg(PrPN-Dpl)(Dpl32)/*Prnp*$^{0/0}$ mice using anti-Dpl FL176 antibodies.**

generation (7–9). However, the mechanism of the antagonistic interaction between PrP^C and Dpl or the truncated PrPs remains to be elucidated.

trans and cis Neuroprotection by the N-terminal Domain of PrP^C against Dpl in Mice—In this study, we showed that PrPN-Dpl (the N-terminal residues 1–124 of PrP^C fused with the residues 58–179 of Dpl) was itself nontoxic and could mitigate the neurotoxicity of wild-type Dpl in Zrch I *Prnp*$^{0/0}$ mice, prolonging the times to the onset of ataxia and Purkinje cell degeneration. Residues 58–179 of Dpl are homologous to residues 125–254 of PrP (10), which encompasses the neurotoxic PrPΔ32–134 peptide. Drisaldi *et al.* (16) showed that Dpl lacking the N-terminal residues 29–49 or 50–90 was still neurotoxic to primary granule cells from Zrch I *Prnp*$^{0/0}$ mice. It is therefore very likely that Dpl-(58–179) is neurotoxic, similarly to the wild-type Dpl in mice devoid of PrP^C. Thus, these results indicate that the N-terminal region of PrP might have neuroprotective potential acting both *cis* and *trans* on Dpl in mice. Interestingly, Rossi *et al.* (28) showed that Zrch II *Prnp*$^{0/0}$ mice, which develop ataxia and Purkinje cell degeneration because of the ectopic expression of Dpl in Purkinje cells, could be rescued by breeding with tga20 mice expressing PrP^C abundantly in the molecular and granule cells but not in Purkinje cells. This suggests that PrP^C expressed by neighboring cells, such as molecular and granule cells, is able to counteract the neurotoxicity of Dpl that is expressed on Purkinje cells and that the *trans* neuroprotection of PrP^C might involve intercellular counteraction against Dpl.

OR Is Dispensable for Neuroprotective Function of PrP^C against Dpl in Mice—In this study, we also showed that PrPΔOR, PrP lacking the OR alone, rescued mice from the ataxia and Purkinje cell degeneration induced by Dpl. This clearly indicates that the OR is unnecessary for PrP^C to antagonize the neurotoxicity of Dpl in mice. Interestingly, Shmerling *et al.* (11) described that the OR is also unnecessary for PrP^C to antagonize the neurotoxicity of truncated PrPs. They showed that granule cell death induced by PrPΔ32–134 could be abrogated by PrPΔ32–93, which lacks the entire OR and about 2/3 of the pre-OR in mice (11). In contrast, in primary cultures of granule cells from Zrch I *Prnp*$^{0/0}$ mice, apoptotic cell death induced by transient overexpression of Dpl could be successfully rescued by wild-type PrP^C but not by PrP lacking the OR (16). Dpl was preferentially toxic to Purkinje cells and not to granule cells in mice (8, 28, 29). Therefore, Dpl toxicity may vary in primary cultured granule cells and mouse models. However, why PrP lacking the OR has differential activity against Dpl in primary cultured granule cells and mice is unknown.

Kuwahara *et al.* (31) showed that hippocampal neuronal cell lines established from *Prnp*$^{0/0}$ mice easily succumbed to apoptosis after serum withdrawal. Furthermore, expression of the anti-apoptotic molecule Bcl-2 could rescue cell lines from apoptosis (31). Bounhar *et al.* (14) also showed that PrP^C prevented human primary neurons from Bax-induced apoptosis. This suggests that the neuroprotective function of PrP^C might involve anti-apoptotic activities. Interestingly, PrP lacking OR failed to rescue the cells from serum withdrawal- and Bax-induced apoptosis, indicating that the OR plays an important role in the anti-apoptotic function of PrP^C (14, 32). Furthermore, our present results showing that PrPΔOR antagonized Dpl in mice clearly indicates that neuroprotection by PrP^C against Dpl is not associated with OR-mediated anti-apoptotic activities.

The anti-apoptotic activity of PrP^C may also be associated with anti-oxidative responses (32, 33). Binding of PrP^C to copper may be important for the anti-oxidative function of PrP^C by either chelating copper or by activating anti-oxidant enzymes, such as Cu,Zn-superoxide dismutase, via transfer of the bound copper to the enzymes, or both (34–36). Six conserved histi-

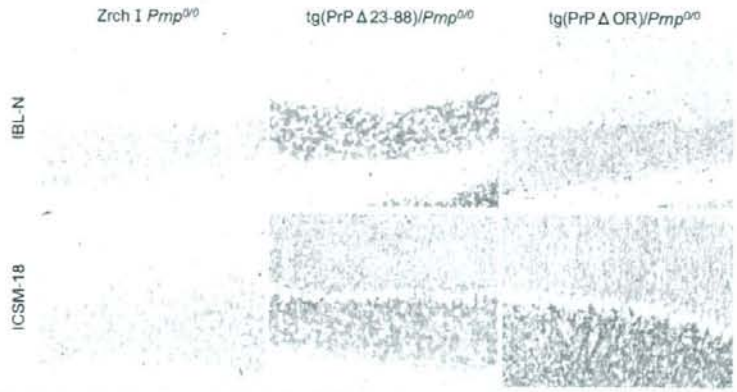

FIGURE 7. **Immunohistochemical analysis of PrPΔ23–88 in the cerebella of mice.** The cerebellar sections from Zrch I *Prnp*$^{0/0}$ mice, tg(PrPΔ23–88)/*Prnp*$^{0/0}$ mice, and tg(PrPΔOR)/*Prnp*$^{0/0}$ mice were subjected to immunohistochemistry using IBL-N and ICSM-18 antibodies, which are directed against PrP residues 24–37 and 146–159, respectively. Magnification, ×20.

dine residues have been identified as copper-binding sites in human PrP^{C}, with four in the OR and two at positions 96 and 111 (37). As PrPΔOR blocked Dpl-mediated neurotoxicity, OR-mediated copper binding might not be involved in the neuroprotection of PrP^{C} against Dpl. In addition, our previous result that PrPΔ23–88, in which two other histidine residues are preserved, failed to rescue mice from ataxia and Purkinje cell degeneration, indicate that copper binding at these sites might not be relevant to the antagonistic function of PrP^{C} against Dpl. Taken together, these suggest that the copper binding-mediated function of PrP^{C}, including anti-oxidative activity, is not associated with its neuroprotective function against Dpl. However, we cannot rule out copper binding to all histidine residues simultaneously for PrP^{C} to have anti-oxidative function.

N-terminal Residues and the Neuroprotective Function of PrP^{C} against Dpl in Mice—In this study, we also showed that PrPΔpreOR, PrP lacking residues 25–50, prevented Dpl-induced ataxia and Purkinje cell degeneration in mice as efficiently as PrPΔOR. This indicates that N-terminal residues 25–50 are not required for PrP^{C} to antagonize Dpl in mice. The two deletions, Δ25–50 and Δ51–90, almost entirely cover the region deleted in PrPΔ23–88, which failed to rescue mice from the neurotoxicity of Dpl (13). PrPΔ23–88 is a chimeric protein of mouse and hamster PrPs, containing two methionines at 108 and 111 in mouse PrP instead of leucine and valine. No such substitutions were present in PrPΔpreOR and PrPΔOR. However, we previously showed that Ngsk *Prnp*$^{0/0}$ mice were successfully rescued from ataxia and Purkinje cell degeneration by full-length chimeric PrP with these methionine substitutions (13), clearly indicating that the incompetence of PrPΔ23–88 to antagonize Dpl is because of lack of residues 23–88 and not to the amino acid substitutions. We also showed here that PrPΔ23–88, PrPΔpreOR, and PrPΔOR were similarly expressed in the cerebellum of mice, consistent with these mutant molecules being expressed under the control of the same hamster PrP promoter/enhancer. Moreover, in this study, we used tg(Dpl32)/*Prnp*$^{0/0}$ mice for the rescue experiments instead of Ngsk *Prnp*$^{0/0}$ mice because tg mice develop ataxia and Purkinje cell degeneration on the Zrch I *Prnp*$^{0/0}$ background much earlier than Ngsk *Prnp*$^{0/0}$ mice because of higher expression of Dpl in their brains (8). Dpl was expressed in tg(Dpl32) mice from the neuron-specific enolase promoter and in Ngsk *Prnp*$^{0/0}$ mice from the residual PrP promoter (4, 8). However, Dpl was similarly expressed in neurons of tg(Dpl32) mice and Ngsk *Prnp*$^{0/0}$ mice with the highest expression in Purkinje cells and hippocampal neurons (4, 8). Therefore, Dpl is toxic to Purkinje cells in the same way in both tg (Dpl32)/*Prnp*$^{0/0}$ mice and Ngsk *Prnp*$^{0/0}$ mice. Taken together, these results indicate that PrPΔpreOR and PrPΔOR but not PrPΔ23–88 can antagonize Dpl neurotoxicity in mice.

PrPΔpreOR and PrPΔOR but not PrPΔ23–88 have the N-terminal two amino acids (residues 23 and 24) conserved adjacent to the junction with the signal peptide. Thus, the two amino acids may be important for the neuroprotection of PrP^{C} against Dpl. This may be consistent with the observation that PrPΔ32–93 protected against the truncated PrPs (11). Interestingly, in PrPΔpreOR the two amino acids are followed by residues starting from 51, generating a new N-terminal sequence (KKPQGGTWG), which is very similar to the N-terminal 9 residues (KKRPKPGGW) of wild-type PrP^{C} and PrPΔ32–93. Six out of 9 of these amino acids are identical. Therefore, this new N-terminal sequence might mimic the function of wild-type PrP^{C}. In PrPΔOR, the N-terminal sequence is intact. Thus, these N-terminal residues might be important for the neuroprotection of PrP^{C} against Dpl. However, it is possible that the antagonistic function of PrP^{C} against Dpl is impaired only by a large deletion of the N-terminal domain with or without the N-terminal residues, as observed in PrPΔ23–88.

Interestingly, PrP with only the central residues 105–125 or 94–134 deleted was reported to be neurotoxic, causing cerebellar degeneration or demyelination in mice, respectively (38, 39). These results suggest that these central residues are essential for PrP^{C} to be neuroprotective. However, PrPΔ23–88 contains these central residues but has no protective activity against Dpl (13). Therefore, the central residues alone might not be enough for PrP^{C} neuroprotectivity, and other region(s), present among the N-terminal residues 23–88, may also be necessary for neuroprotection. These region(s) might be located in the N-terminal 2 or 9 residues. However, unrelated region(s) to the N-terminal 2 or 9 residues may also be necessary.

Possible Mechanisms for N-terminal Region Neuroprotectivity of PrP^{C} against Dpl—There are reports showing that the N-terminal domain is involved in the subcellular trafficking of PrP^{C} (40–44). In this study, we found that PrPΔ23–88, PrPΔpreOR, and PrPΔOR were expressed in the molecular and granule cell layers of the cerebellum and on the cell surface of COS-7 monkey kidney cells similarly to that in wild-type PrP^{C}.

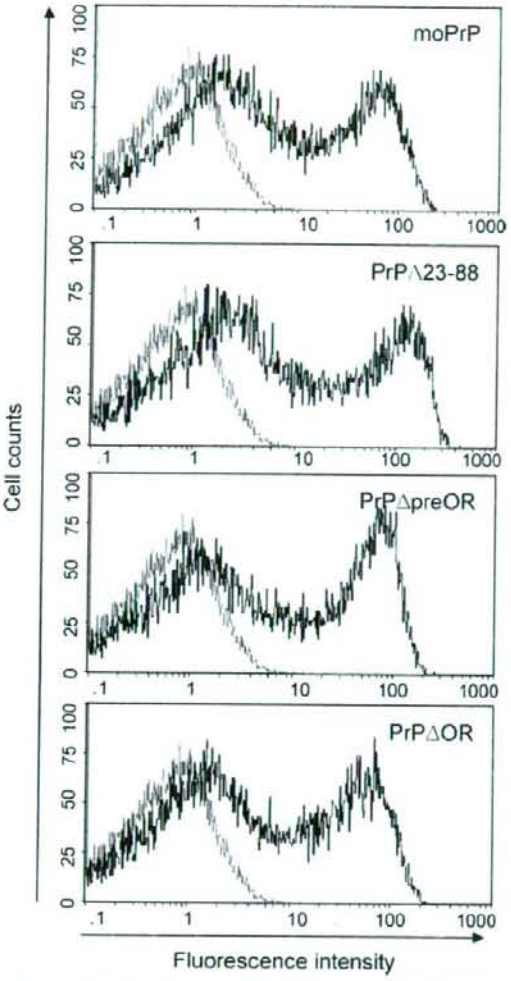

FIGURE 8. **Cell surface expression of PrP mutants.** COS-7 cells were transiently transfected with expression vectors encoding wild-type mouse PrP^C, PrPΔpreOR, PrPΔOR, and PrPΔ23–88 and subjected to flow cytometry analysis using SAF61 antibodies 48 h after transfection. All PrP mutants were expressed on the cell surface similarly to wild-type PrP^C. *Gray* and *black lines* indicate cells transfected with pcDNA3.1 vector alone and pcDNA3.1 carrying cDNA corresponding wild-type PrP^C, PrPΔpreOR, PrPΔOR, or PrPΔ23–88.

This indicates that the cellular expression and cell surface transport of these mutant molecules may be unchanged. It is therefore unlikely that the cell surface localization of PrPΔ23–88 is different from that of PrPΔpreOR and PrPΔOR because of the large deletion of the N-terminal domain, thus impairing the neuroprotective function of PrP^C. The N-terminal part is also involved in efficiency of PrP^C endocytosis. PrPΔ23–90 and PrPΔ48–93, which lacks the OR region, were shown not to be efficiently internalized in mouse neuroblastoma N2a cells (44), indicating that lack of the OR alone might affect the internalization of PrP^C. However, we showed here that PrPΔOR was neuroprotective against Dpl in mice, indicating that the internalization may not be relevant to the neuroprotective activity of PrP^C. Recently, Santuccione *et al.* (45) showed that PrP^C activates $p59^{Fyn}$ to enhance neurite outgrowth via recruitment of the neuronal cell adhesion molecule to lipid rafts, indicating that the proper localization at lipid rafts could be important for PrP^C function. Interestingly, PrPΔ23–90 but not PrP lacking the OR region was not properly targeted to lipid rafts (44). Thus, PrPΔ23–88 but not PrPΔOR and PrPΔpreOR may not properly localize at lipid rafts either because of lack of the N-terminal 2 or 9 residues or because of large scale deletion of the N-terminal domain with or without the N-terminal residues, resulting in unsuccessful rescue of mice from Dpl neurotoxicity.

Alternatively, the N-terminal region may be involved in the neuroprotective function of PrP^C by eliciting a neuroprotective signal through an associated molecule, as in the models proposed so far (11, 30, 38, 39, 46). Among them, Weissmann and Aguzzi (46) proposed that PrP^C binds to an as yet unidentified molecule and elicits a Purkinje cell survival signal through the N-terminal domain. Dpl can bind to the molecule but cannot generate the signal because of lack of the N-terminal domain, resulting in Purkinje cell degeneration. However, PrP^C competes with Dpl for the molecule, thereby preventing Dpl-induced Purkinje cell degeneration. The results showing that PrPN-Dpl, PrPΔpreOR, and PrPΔOR but not PrPΔ23–88 antagonize the neurotoxicity of Dpl suggests that the former three molecules bind the molecule and produce the survival signal through the N-terminal domain of PrP^C, preventing neurodegeneration. This may be because they have a part of or the whole N-terminal domain. It might be also possible that Dpl itself may bind to its own unidentified cognate molecule to elicit a neurotoxic signal and PrP^C, PrPN-Dpl, PrPΔpreOR, and PrPΔOR but not PrPΔ23–88 may compete for the molecule via a part of or the whole N-terminal domain, thereby preventing Dpl-mediated neurotoxicity. However, these models can be verified only if the hypothetical molecules are identified.

In this study, we showed that the N-terminal domain mediates the neuroprotective function of PrP^C against Dpl in *trans* and *cis* and that the OR region and residues 25–50 (pre-OR) are dispensable for the neuroprotective function of PrP^C. However, to understand the exact molecular mechanism how the N-terminal domain is involved in the neuroprotective function of PrP^C, further studies are required.

Acknowledgments—We thank Prof. Stanley B. Prusiner and Dr. Patrick Tremblay for providing Zrch I $Prnp^{0/0}$ mice.

REFERENCES

1. Oesch, B., Westaway, D., Walchli, M., McKinley, M. P., Kent, S. B., Aebersold, R., Barry, R. A., Tempst, P., Teplow, D. B., Hood, L. E., Prusiner, S. B., and Weissmann, C. (1985) *Cell* **40,** 735–746
2. Prusiner, S. B. (1998) *Proc. Natl. Acad. Sci. U. S. A.* **95,** 13363–13383
3. Prusiner, S. B. (1997) *Science* **278,** 245–251
4. Li, A., Sakaguchi, S., Atarashi, R., Roy, B. C., Nakaoke, R., Arima, K., Okimura, N., Kopacek, J., and Shigematsu, K. (2000) *Cell. Mol. Neurobiol.* **20,** 553–567
5. Moore, R. C., Lee, I. Y., Silverman, G. L., Harrison, P. M., Strome, R., Heinrich, C., Karunaratne, A., Pasternak, S. H., Chishti, M. A., Liang, Y., Mastrangelo, P., Wang, K., Smit, A. F., Katamine, S., Carlson, G. A., Cohen, F. E., Prusiner, S. B., Melton, D. W., Tremblay, P., Hood, L. E., and West-

away, D. (1999) *J. Mol. Biol.* **292,** 797–817
6. Li, A., Sakaguchi, S., Shigematsu, K., Atarashi, R., Roy, B. C., Nakaoke, R., Arima, K., Okimura, N., Kopacek, J., and Katamine, S. (2000) *Am. J. Pathol.* **157,** 1447–1452
7. Moore, R. C., Mastrangelo, P., Bouzamondo, E., Heinrich, C., Legname, G., Prusiner, S. B., Hood, L., Westaway, D., DeArmond, S. J., and Tremblay, P. (2001) *Proc. Natl. Acad. Sci. U. S. A.* **98,** 15288–15293
8. Yamaguchi, N., Sakaguchi, S., Shigematsu, K., Okimura, N., and Katamine, S. (2004) *Biochem. Biophys. Res. Commun.* **319,** 1247–1252
9. Anderson, L., Rossi, D., Linehan, J., Brandner, S., and Weissmann, C. (2004) *Proc. Natl. Acad. Sci. U. S. A.* **101,** 3644–3649
10. Mo, H., Moore, R. C., Cohen, F. E., Westaway, D., Prusiner, S. B., Wright, P. E., and Dyson, H. J. (2001) *Proc. Natl. Acad. Sci. U. S. A.* **98,** 2352–2357
11. Shmerling, D., Hegyi, I., Fischer, M., Blattler, T., Brandner, S., Gotz, J., Rulicke, T., Flechsig, E., Cozzio, A., von Mering, C., Hangartner, C., Aguzzi, A., and Weissmann, C. (1998) *Cell* **93,** 203–214
12. Flechsig, E., Hegyi, I., Leimeroth, R., Zuniga, A., Rossi, D., Cozzio, A., Schwarz, P., Rulicke, T., Gotz, J., Aguzzi, A., and Weissmann, C. (2003) *EMBO J.* **22,** 3095–3101
13. Atarashi, R., Nishida, N., Shigematsu, K., Goto, S., Kondo, T., Sakaguchi, S., and Katamine, S. (2003) *J. Biol. Chem.* **278,** 28944–28949
14. Bounhar, Y., Zhang, Y., Goodyer, C. G., and LeBlanc, A. (2001) *J. Biol. Chem.* **276,** 39145–39149
15. Sakudo, A., Lee, D. C., Saeki, K., Nakamura, Y., Inoue, K., Matsumoto, Y., Itohara, S., and Onodera, T. (2003) *Biochem. Biophys. Res. Commun.* **308,** 660–667
16. Drisaldi, B., Coomaraswamy, J., Mastrangelo, P., Strome, B., Yang, J., Watts, J. C., Chishti, M. A., Marvi, M., Windl, O., Ahrens, R., Major, F., Sy, M. S., Kretzschmar, H., Fraser, P. E., Mount, H. T., and Westaway, D. (2004) *J. Biol. Chem.* **279,** 55443–55454
17. Brinster, R. L., Chen, H. Y., Trumbauer, M. E., Yagle, M. K., and Palmiter, R. D. (1985) *Proc. Natl. Acad. Sci. U. S. A.* **82,** 4438–4442
18. Wilmut, I., Hooper, M. L., and Simons, J. P. (1991) *J. Reprod. Fertil.* **92,** 245–279
19. Bueler, H., Fischer, M., Lang, Y., Bluethmann, H., Lipp, H. P., DeArmond, S. J., Prusiner, S. B., Aguet, M., and Weissmann, C. (1992) *Nature* **356,** 577–582
20. Scott, M. R., Kohler, R., Foster, D., and Prusiner, S. B. (1992) *Protein Sci.* **1,** 986–997
21. Liu, T., Zwingman, T., Li, R., Pan, T., Wong, B. S., Petersen, R. B., Gambetti, P., Herrup, K., and Sy, M. S. (2001) *Brain Res.* **896,** 118–129
22. Barmada, S., Piccardo, P., Yamaguchi, K., Ghetti, B., and Harris, D. A. (2004) *Neurobiol. Dis.* **16,** 527–537
23. Watts, J. C., Drisaldi, B., Ng, V., Yang, J., Strome, B., Horne, P., Sy, M. S., Yoong, L., Young, R., Mastrangelo, P., Bergeron, C., Fraser, P. E., Carlson, G. A., Mount, H. T., Schmitt-Ulms, G., and Westaway, D. (2007) *EMBO J.* **26,** 4038–4050
24. McLennan, N. F., Brennan, P. M., McNeill, A., Davies, I., Fotheringham, A., Rennison, K. A., Ritchie, D., Brannan, F., Head, M. W., Ironside, J. W., Williams, A., and Bell, J. E. (2004) *Am. J. Pathol.* **165,** 227–235
25. Sakurai-Yamashita, Y., Sakaguchi, S., Yoshikawa, D., Okimura, N., Masuda, Y., Katamine, S., and Niwa, M. (2005) *Neuroscience* **136,** 281–287
26. Weise, J., Crome, O., Sandau, R., Schulz-Schaeffer, W., Bahr, M., and Zerr, I. (2004) *Neurosci. Lett.* **372,** 146–150
27. Hoshino, S., Inoue, K., Yokoyama, T., Kobayashi, S., Asakura, T., Teramoto, A., and Itohara, S. (2003) *Acta Neurochir. Suppl.* **86,** 297–299
28. Rossi, D., Cozzio, A., Flechsig, E., Klein, M. A., Rulicke, T., Aguzzi, A., and Weissmann, C. (2001) *EMBO J.* **20,** 694–702
29. Sakaguchi, S., Katamine, S., Nishida, N., Moriuchi, R., Shigematsu, K., Sugimoto, T., Nakatani, A., Kataoka, Y., Houtani, T., Shirabe, S., Okada, H., Hasegawa, S., Miyamoto, T., and Noda, T. (1996) *Nature* **380,** 528–531
30. Behrens, A., and Aguzzi, A. (2002) *Trends Neurosci.* **25,** 150–154
31. Kuwahara, C., Takeuchi, A. M., Nishimura, T., Haraguchi, K., Kubosaki, A., Matsumoto, Y., Saeki, K., Yokoyama, T., Itohara, S., and Onodera, T. (1999) *Nature* **400,** 225–226
32. Sakudo, A., Lee, D. C., Nishimura, T., Li, S., Tsuji, S., Nakamura, T., Matsumoto, Y., Saeki, K., Itohara, S., Ikuta, K., and Onodera, T. (2005) *Biochem. Biophys. Res. Commun.* **326,** 600–606
33. Brown, D. R., Nicholas, R. S., and Canevari, L. (2002) *J. Neurosci. Res.* **67,** 211–224
34. Haigh, C. L., and Brown, D. R. (2006) *J. Neurochem.* **98,** 677–689
35. Brown, D. R., Qin, K., Herms, J. W., Madlung, A., Manson, J., Strome, R., Fraser, P. E., Kruck, T., von Bohlen, A., Schulz-Schaeffer, W., Giese, A., Westaway, D., and Kretzschmar, H. (1997) *Nature* **390,** 684–687
36. Brown, D. R., Schulz-Schaeffer, W. J., Schmidt, B., and Kretzschmar, H. A. (1997) *Exp. Neurol.* **146,** 104–112
37. Jackson, G. S., Murray, I., Hosszu, L. L., Gibbs, N., Waltho, J. P., Clarke, A. R., and Collinge, J. (2001) *Proc. Natl. Acad. Sci. U. S. A.* **98,** 8531–8535
38. Li, A., Christensen, H. M., Stewart, L. R., Roth, K. A., Chiesa, R., and Harris, D. A. (2007) *EMBO J.* **26,** 548–558
39. Baumann, F., Tolnay, M., Brabeck, C., Pahnke, J., Kloz, U., Niemann, H. H., Heikenwalder, M., Rulicke, T., Burkle, A., and Aguzzi, A. (2007) *EMBO J.* **26,** 538–547
40. Pauly, P. C., and Harris, D. A. (1998) *J. Biol. Chem.* **273,** 33107–33110
41. Shyng, S. L., Moulder, K. L., Lesko, A., and Harris, D. A. (1995) *J. Biol. Chem.* **270,** 14793–14800
42. Taylor, D. R., Watt, N. T., Perera, W. S., and Hooper, N. M. (2005) *J. Cell Sci.* **118,** 5141–5153
43. Nunziante, M., Gilch, S., and Schatzl, H. M. (2003) *J. Biol. Chem.* **278,** 3726–3734
44. Walmsley, A. R., Zeng, F., and Hooper, N. M. (2003) *J. Biol. Chem.* **278,** 37241–37248
45. Santuccione, A., Sytnyk, V., Leshchyns'ka, I., and Schachner, M. (2005) *J. Cell Biol.* **169,** 341–354
46. Weissmann, C., and Aguzzi, A. (1999) *Science* **286,** 914–915